Journal of the Korean Society of Surveying, Geodesy, Photogrammetry and Cartography
Vol. 37, No. 5, 367-377, 2019
https://doi.org/10.7848/ksgpc.2019.37.5.366

ISSN 1598-4850(Print)
ISSN 2288-260X(Online)
Original article

Development and Performance Analysis of a New Navigation Algorithm by Combining Gravity Gradient and Terrain Data as well as EKF and Profile Matching

Lee, Jisun [1] · Kwon, Jay Hyoun [2]

Abstract

As an alternative navigation system for the non-GNSS (Global Navigation Satellite System) environment, a new type of DBRN (DataBase Referenced Navigation) which applies both gravity gradient and terrain, and combines filter-based algorithm with profile matching was suggested. To improve the stability of the performance compared to the previous study, both centralized and decentralized EKF (Extended Kalman Filter) were constructed based on gravity gradient and terrain data, and one of filters was selected in a timely manner. Then, the final position of a moving vehicle was determined by combining a position from the filter with the one from a profile matching. In the simulation test, it was found that the overall performance was improved to the 19.957m by combining centralized and decentralized EKF compared to the centralized EKF that of 20.779m. Especially, the divergence of centralized EKF in two trajectories located in the plain area disappeared. In addition, the average horizontal error decreased to the 16.704m by re-determining the final position using both filter-based and profile matching solutions. Of course, not all trajectories generated improved performance but there is not a large difference in terms of their horizontal errors. Among nine trajectories, eights show smaller than 20m and only one has 21.654m error. Thus, it would be concluded that the endemic problem of performance inconsistency in the single geophysical DB or algorithm-based DBRN was resolved because the combination of geophysical data and algorithms determined the position with a consistent level of error.

Keywords : Gravity Gradient, Terrain, Centralized Extended Kalman Filter, Decentralized Extended Kalman Filter, Profile Matching, Combination of Database and Algorithm

1. Introduction

An alternative navigation system is becoming an issue for solving the accuracy degradation problem from signal blockages or solar storms in satellite-based navigation systems. A typical alternative navigation system combines an INS (Inertial Navigation System) with other external sensors. Because the INS error increases as time goes on, a combined navigation system compensates for the INS error and determines accurate positions of a vehicle over a long period of time. One such GNSS/INS (Global Navigation Satellite System / INS) has been studied since the middle of the 1950s (Cox, 1978; Nielson *et al.*, 1986), but its positional accuracy decreases dramatically in non-GNSS environments. Thus, another type of alternative system, called DBRN (DataBase Referenced Navigation), combines an INS with geophysical sensors and a DB and is being studied due to development of sensors with high precision and resolution. A submarine cannot receive a GNSS signal when it operates underwater, so the necessity for DBRN is especially emphasized (Stutters *et al.*, 2008; Leonard and Bahr, 2019).

The early stage of research on DBRN generally applied

Received 2019. 09. 30, Revised 2019. 10. 12, Accepted 2019. 10. 18
1) Member, Dept. of Geoinformatics, University of Seoul (E-mail : leejs@uos.ac.kr)
2) Corresponding Author, Member, Dept. of Geoinformatics, University of Seoul (E-mail : jkwon@uos.ac.kr)

single geophysical data (e.g. terrain, gravity) or a navigation algorithm (e.g. a filter, or profile matching) (Hollowell, 1990; Laur and Llanso, 1995; Zhang *et al*., 2004; Cowie *et al*., 2008; Richeson, 2008; Wang and Bian, 2008; Rogers, 2009; Liu *et al*., 2010; DeGregoria, 2010). However, positional accuracy was not at a satisfactory level, because the INS error was not properly compensated for when a vehicle moved over a plain. In addition, both the divergence problem of a filter-based algorithm and the relatively lower positional accuracy in the profile-matching algorithm were pointed out (Perea *et al*., 2007; Groves, 2013; Lee *et al*., 2014). Thus, recent studies have focused on the combination of various geophysical sensors/DBs and navigation algorithms to complement the weakness and improve accuracy (Robins, 1998; Liu *et al*., 2009; Xiong *et al*., 2013; Wang *et al*., 2016; Yurong *et al*., 2016; Dai *et al*., 2019). The studies on DBRN started in the middle of the 2000s in Korea (Lee and Kwon, 2010; Mok et al., 2012; Lee *et al*., 2013; Yu *et al*., 2013; Lee *et al*., 2015). Those studies also faced similar problems, and accuracy remained at about the 30–50m level. Thus, a combination of geophysical sensors/DBs or navigation algorithms was suggested in mid-2010 as a way to improve accuracy. Lee and Kwon (2016) combined the terrain and gravity gradient data in a centralized EKF (Extended Kalman Filter), and the final position was re-determined by combining the filter and profile matching every 10 seconds. However, some tested trajectories show better positional accuracy when single geophysical data and a navigation algorithm was applied, so the development of a decentralized EKF or switching of the navigation algorithm were suggested for an improvement plan.

As a follow-up study by Lee and Kwon (2016), a new navigation algorithm that combines heterogeneous geophysical data and sensors was proposed, and its positional accuracy was evaluated based on simulation. In detail, a decentralized EKF was developed, and switching between a centralized EKF and a decentralized EKF was tested. Also, final positions were determined by combining or switching the EKF solution with profile matching.

2. Methodologies

The reason to combine heterogeneous geophysical DBs and algorithms is to complement the weakness in the use of a single DB or algorithm, and to improve accuracy and stability. For example, terrain data show higher accuracy and resolution compared to the gravity gradient data in the same target area. Only terrain height is extracted from the terrain DB, but six components are available from gravity gradient DBs. It means that GGRN (Gravity Gradient Referenced Navigation) can be more stable than TRN (Terrain Referenced Navigation) when a vehicle moves over a low variation area. In addition, the filter-based navigation algorithm that compensates for the INS error every epoch sometimes diverges when the local variation in geophysical data is irregular. In this situation, the profile-matching algorithm that stacks geophysical information for a while and compares it to find the optimal position could determine the position with high accuracy. Thus, a combination of geophysical data and algorithms is necessary to guarantee stability anywhere the vehicle moves.

In this study, both the terrain and gravity gradient data were combined with a filter-based algorithm, and the final position was determined by a solution from the filter with profile matching. In a previous study, the terrain and gravity gradient were included as measurements in the centralized EKF. However, independent GGRN and TRN were operated and combined as a type of decentralized EKF for this study, and switching between a centralized EKF and a decentralized EKF was considered. Also, a profile matching algorithm was applied to check the reliability of the EKF solution, and the final position was determined by combining or switching two solutions from the EKF and profile matching. When updating the position, the P matrix of the EKF was updated by multiplying a constant, considering the method of final position determination. Figure 1 illustrates the concept of the new navigation algorithm that combines heterogeneous geophysical data and algorithms. In the figure, the explanation in red is the part improved, compared to the previous study.

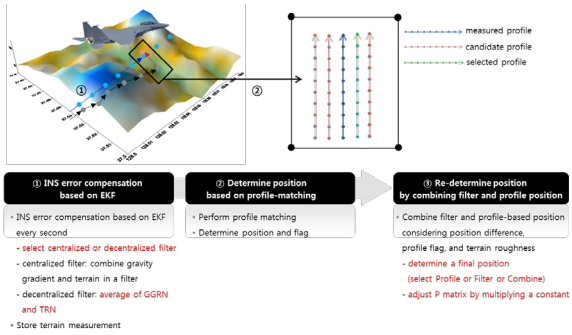

Fig. 1. Principles for combining a heterogeneous geophysical DB and algorithms

2.1 Combination of terrain and gravity gradient using an EKF

The filter-based algorithm compensates for the INS error by applying the difference between the information obtained by sensors and that extracted from the DB as a filter measurement. Among the various filters, e.g. EKF, UKK (Unscented Kalman Filter), BKF (Bank of Kalman Filter), the PMF (Point Mass Filter), etc., the EKF is broadly applied due to its fast processing time. However, an EKF assumes that the relationship between measurement and states (INS error) is linear, so it sometimes diverges when the linearity is not guaranteed on a plain or irregular-variation area. Geophysical data do not generally change to the specific positional direction, and thus, over-correction or a wrong correction can frequently occur in the EKF. Although sensors and DBs with higher accuracy and resolution are available in TRN, stability dramatically decreases in some test areas, compared to GGRN. That is because TRN applies only one height difference for the EKF measurement, whereas GGRN applies six components. Thus, a combination of terrain and gravity gradients is required to improve the stability of the EKF. There are two ways to combine them: the centralized type and the decentralized. The centralized EKF stacks all available geophysical information differences in a measurement vector and estimates the INS error. On the other hand, the decentralized EKF constructs an independent local filter based on single geophysical data, and combines the solution in a master filter. In general, a centralized filter has the benefit of minimal information loss (Skog, 2009), so the centralized type was selected in the previous study (Lee and Kwon (2016)). In a simulation test, improved positional accuracy was achieved by combining terrain and gravity gradient data, but the divergence problem was not figured out in two tested trajectories.

Thus, the centralized EKF and decentralized EKF were constructed at the same time, and the final solution from the filter-based algorithm was determined by averaging or switching, considering the difference in estimated position and the local characteristics of the geophysical data. The strategy to combine centralized and decentralized EKFs is summarized in Table 1. When the positional difference between the estimated position from the EKFs is smaller than half of the positional precision extracted from the P matrix, selection of a solution from the filter does not have a huge effect on the navigation result. Thus, the average of centralized and decentralized EKFs was applied; but the local roughness of geophysical data was additionally checked to improve the stability. The limit to check local roughness for the terrain is 20m of standard deviation, while 1Eo and 6Eo were applied for the average and standard deviation in the gravity gradient. On the other hand, the centralized EKF generates relatively stable results, especially with a large positional difference or lower variations in the geophysical data. Thus, the INS error was compensated for by applying the estimate from the centralized EKF, and the P matrix was adjusted. If GGRN and TRN have a small positional difference, but their local characteristics are large enough, the position from the centralized filter could have a bias. In that case, the estimates from the centralized EKF were applied, but the position part of the P matrix was degraded by multiplying the original P matrix by 1.1 to reflect the ambiguity of the EKF solution.

2.2 Profile matching algorithm

The reason to combine profile matching with EKF is to complement the over-correction or wrong correction problem when the linearity between measurements and states is not guaranteed in the EKF. In general, the success rate and the stability of profile matching are high when a vehicle moves in a region where the geophysical data vary a lot. Therefore, profile matching would be applied to check the reliability of the estimates from the EKF as well as to bind the position

Table 1. The standard to combine a centralized EKF and a decentralized EKF

Condition 1	Condition 2/3		Combination	P matrix
Both ② and ③ < Ppos_cent/2	Both gravity gradient and terrain change sufficiently		1:1 (average)	Pgg
	Either gravity gradient or terrain shows low variation		Centralized	Pcent
② or ③ > Ppos_cent/2	① < Ppos_cent/2	Both gravity gradient and terrain change sufficiently	Centralized	Pcent x 1.1
		Either gravity gradient or terrain shows low variation	Centralized	Pcent
	① > Ppos_cent/2		Centralized	Pcent

Position difference
① Estimated position difference between GGRN and TRN (decentralized filter)
② Estimated position difference between centralized EKF and GGRN
③ Estimated position difference between centralized EKF and TRN

error. For this reason, profile matching was constructed and applied in this study. Among the various geophysical data, terrain data were selected because the resolution and accuracy of sensors and DBs are higher than gravity gradient.

In the profile matching, a number of candidate profiles were generated in the test area, and the final INS position was selected when the difference between stacked terrain information (the height of a vehicle profile) and extracted information from the DB (the height from a candidate profile) is small. To remove the effect of the sign in the difference computation, the differences were changed to absolute values, called the MAD (Mean Absolute Difference). Since the performance of profile matching is better when the terrain varies a lot, two indicators called σ_T and σ_Z were considered. For reference, σ_T is the standard deviation of the height difference between the vehicle and the candidate profile; σ_Z is the standard deviation of the height difference when the height difference was already calculated in each profile. In addition, selection of a candidate profile showing the minimum MAD is quite risky due to errors in DBs and sensors. Therefore, three top-ranked candidate profiles were extracted, and the MAD ratio was checked to improve stability. Finally, the INS position was determined by averaging two candidates or selecting one from the profile matching, and a flag was allocated to show the reliability of the selection. Among four types of flag, flags 10 and 11 do not have sufficient reliability to update the INS position, but the selection could be used to compare with a solution from the EKF, so they were referenced in the combination of EKF and profile matching. Please see detailed strategies for profile matching in Lee and Kwon (2016).

Table 2. The standard to determine the position and flag in the profile matching algorithm

flag	Condition	Final position
1	MAD of the top-priority candidate profile is small (the MAD ratio is smaller than 80%)	Top-priority candidate profile
2	MAD of the top two candidate profiles are similar (the ratio between two MADs is over 80%), but the position difference is less than 135m	Average of two top candidate profiles
11	MAD of the top two candidate profiles are similar (the ratio between two MADs is over 80%), but the position difference is greater than 135m	Top-priority candidate profile (low reliability)
10	MAD of the top three candidate profiles are similar	

2.3 Combination of navigation algorithms (EKF and profile matching)

EKF estimates the INS position every second, whereas profile matching determines the position every 10 seconds. Thus, the determination of the final position by combining two navigation algorithms was performed every 10 seconds. It means that the INS errors are compensated for every second, and a new position is determined by combining or switching EKF and profile matching solutions every 10 seconds.

In the previous study, two candidates (one from the centralized EKF and the other from profile matching) were combined by applying a weight, and the P matrix of the filter was updated by allocating a specific value (e.g. 45m, 90m, etc.) to the profile matching. In that case, a relatively large error could be allocated, although the profile matching generates reliable position information. Because the newly proposed filter-based algorithm combines centralized and decentralized EKFs to improve stability, the estimated P matrix in the filter was assumed to be trustworthy. Instead, the position part of the P matrix was slightly adjusted by multiplying a constant (e.g. 1.1, 1.2) to reflect the ambiguity in case the profile matching solution is applied to determine a new solution. In addition, the previous study set up detailed conditions in the combination of the navigation algorithms, considering the flag of the profile matching as one of the main factors. However, the new combination algorithm checks whether the flag is 1 or 2, and the terrain roughness indicators are handled meaningfully.

The conditions to combine navigation algorithms are summarized in Table 3, and the final position is determined considering weight. In general, the EKF-based solution has higher accuracy, so the weight of the EKF is relatively larger than the weight of profile matching. However, the weight of the EKF was adjusted to be similar to the weight of profile matching when the position from profile matching is trusted, in order to make the relatively large effect of the profile matching on the final solution. When W_{filter} is 1 and $W_{profile}$ means the position from the EKF was totally applied. In the case of the P matrix, the original P matrix estimated from the EKF was applied for cases that do not have any comments. For reference, the standard to check the positional difference between navigation algorithms (e.g. 100m, 120m, 180m) were calculated by multiplying a constant with the 20m estimated position error of the combined EKFs. Because of inconsistency in geophysical data and algorithms, the multiplier was determined empirically based on numerous simulation tests to determine the value that fits generally. Again, those values were determined in order to find the most suitable value. Eq. (1) shows the combination strategy for the EKF and profile matching.

$$\begin{aligned} \phi_{new} &= (W_{filter} \times \phi_{filter} + W_{profile} \times \phi_{profile})/(W_{filter} + W_{profile}) \\ \lambda_{new} &= (W_{filter} \times \lambda_{filter} + W_{profile} \times \lambda_{profile})/(W_{filter} + W_{profile}) \\ P_{pos\_new} &= (W_{filter} \times P_{pos\_filter} + W_{profile} \times P_{pos\_profile})/(W_{filter} + W_{profile}) \end{aligned} \quad (1)$$

Table 4. The standard to combine filter-based algorithms and the profile matching algorithm

Condition			New Position and P matrix
$\phi_{filter} - \phi_{profile} < 20m$ $\lambda_{filter} - \lambda_{profile} < 20m$	profile flag = 1 or 2		$W_{filter} = 0, W_{profile} = 1$
	else		$W_{filter} = 1, W_{profile} = 1$
$\phi_{filter} - \phi_{profile} > 180m$ or $\lambda_{filter} - \lambda_{profile} > 180m$			$W_{filter} = 1, W_{profile} = 0$ $P_{pos\_new} = P_{pos\_filter} \times 1.3$
else	$\sigma_T > 30m$ $\sigma_Z > 15m$	$\phi_{filter} - \phi_{profile} < 100m$ $\lambda_{filter} - \lambda_{profile} < 100m$ or profile flag = 1 or 2	$W_{filter} = 3,\ W_{profile} = 1$ $P_{pos\_new} = P_{pos\_filter} \times 1.2$
		else	$W_{filter} = 5,\ W_{profile} = 1$ $P_{pos\_new} = P_{pos\_filter} \times 1.3$
	else	$\phi_{filter} - \phi_{profile} < 100m$ $\lambda_{filter} - \lambda_{profile} < 100m$	$W_{filter} = 10,\ W_{profile} = 1$ $P_{pos\_new} = P_{pos\_filter} \times 1.2$
		else	$W_{filter} = 1,\ W_{profile} = 0$ $P_{pos\_new} = P_{pos\_filter} \times 1.3$

3. Performance Analysis of Combining Geophysical DBs and Algorithms

3.1 Simulation Environments

The performance of the newly proposed combination algorithm was evaluated based on simulation tests. In the simulation, the vehicle flies loaded with a navigation-grade IMU (Inertial Measurement Unit), a FTG (Full Tensor Gradiometer) with a 3Eo level of precision, and a radar altimeter with 5m precision. Also, two complementary sensors, a barometer, and a compass were added to compensate for the altitude and yaw error of the IMU. In terms of a geophysical DB, one terrain DB and six gravity gradient DBs were loaded, and their resolution and precision were assumed as listed in Table 5, considering the currently available sensors and DBs. In practical terms, both the radar altimeter and the barometer are necessary to determine the terrain height, such that the measurement error of the sensor in TRN was assumed to be 10m.

The performance was checked in a total of nine trajectories that were generated from south to north with a 0.25° interval from longitude 127° to 129°. The starting position of each trajectory was 35°, and the left seven trajectories finished the flight at 38°, but the right two trajectories ended at 37.5° because the ocean is located in the northeast part of Korea. The flight altitude was assumed to be 3000m, and the vehicle speed was 350km/h.

3.2 Performance Analysis

The performance of the new navigation algorithm has been evaluated in two parts. The update effect from the centralized EKF to the decentralized EKF was verified in the first test, and the combining of decentralized EKF with the profile matching was followed. In the performance analysis, the horizontal position accuracy means the standard deviation of horizontal position error with respect to the true trajectory, as shown in Eq. (2).

$$S_{Horizontal} = \sqrt{\frac{\sum(\Delta d - \widehat{\Delta d})^2}{n-1}} \tag{2}$$

where, Δd is the horizontal position error which is calculated by the sum of differences between positions estimated from the combination algorithm and true trajectory, and $\widehat{\Delta d}$ is mean of the horizontal position error, respectively, and n is the total number of epochs.

3.2.1 Combination of centralized and decentralized EKFs

The horizontal position accuracy of the newly developed combined EKF is summarized in Table 6. To compare the effect of the new algorithm, the single geophysical referenced navigation (GGRN, TRN), and centralized filter accuracy, which were published in Lee and Kwon (2016), are included. Because currently available sensors and DBs were assumed in the simulation, the average horizontal accuracy of GGRN and TRN remained about 115m and 54m, respectively. It should be mentioned that two diverged trajectories were excluded when calculating the average from TRN. The reason for the divergence was found to be the vehicle starting the flight in a quite smooth region. To figure out the divergence problem, Lee and Kwon (2016) developed GGTRN (Gravity Gradient and Terrain Referenced Navigation) through a centralized EKF. The average decreased to the 21m level, but the divergence problem was not solved. However, it was found that horizontal error in trajectories 8 and 9 decreased to less than 50m with the newly proposed algorithm (centralized + decentralized EKF). Also, the average horizontal error decreased to 19.957m. Again, it should be emphasized that 19.957m is the average that was calculated based on all the trajectories.

Table 5. Specifications of the DB and sensors for GGRN and TRN

GGRN			TRN		
DB resolution (arcsec)	DB precision (Eo)	Sensor precision (Eo)	DB resolution (arcsec)	DB precision (m)	Sensor precision (m)
30	3	3	3	16	10

Of course, not all trajectories showed improvement from the combination of centralized and decentralized EKFs. For example, trajectories 3 and 4 had the smallest horizontal error in TRN, and trajectory 7 showed the minimum error in GGTRN (centralized). However, TRN did not have consistent results, because the range was from 7.2m to divergence. Also, the centralized filter was not the optimal solution to solve the divergence problem. On the other hand, the newly proposed algorithm shows a uniform distribution, and maximum error was bound smaller than 50m, so the new algorithm is meaningful in terms of stability.

3.2.2 Combination of GGTRN(centralized+decentralized) and profile matching

Before showing the performance from the combination of navigation algorithms, the horizontal position error is summarized in Table 7. The average horizontal error for all trajectories was calculated at about 67m, and no divergence occurred, so horizontal error does not exceed 100m in trajectories 8 and 9. Overall performance was better in the EKF, but profile matching is sufficient to check the reliability of the EKF and to determine new update conditions, because it generates consistent results. The profile matching algorithm was developed in Lee and Kwon (2016); thus, please refer to their initial results and their analysis of the combination possibility between heterogeneous algorithms.

Table 8 shows the navigation performance when the EKFs (centralized + decentralized) and profile matching were combined. Among the nine trajectories, horizontal error decreased in trajectories 1, 5, 6, 8, and 9. The largest improvement (about 318%) was found in trajectory 8; the 46.130m position error from the EKF (centralized+decentralized) was bound to 14.505m when the profile matching was combined. On the other hand, trajectories 2, 3, 4, and 7 showed poorer navigation results than EKF alone, and the maximum degradation was about 4.8m. The horizontal error in trajectory 3 increased from 12.104m to 16.872m. However, the average for all the

Table 6. Horizontal errors of the filter-based algorithms (GGRN, TRN, GGTRN(centralized), GGTRN(centralized+decentralized))

Traj. no.	GGRN (m)	TRN (m)	GGTRN (centralized) (m)	GGTRN (centralized + decentralized) (m)
1	192.337	22.821	63.714	18.247
2	192.678	294.579	22.630	15.094
3	52.727	11.092	10.985	12.104
4	41.972	9.577	9.847	13.577
5	187.572	7.199	8.644	16.007
6	71.020	15.058	16.310	14.967
7	87.817	16.227	13.321	15.929
8	141.560	36976.350	4472.651	46.130
9	64.557	8272.175	1004.115	27.560
Average	114.693	53.793*	20.779*	19.957

* the average horizontal error when the trajectory showing divergence is excluded

Table 7. Horizontal errors of the profile matching algorithm (Lee and Kwon (2016))

Traj. no.	1	2	3	4	5
Horizontal error (m)	66.438	90.555	65.529	49.100	40.391
Traj. no.	6	7	8	9	average
Horizontal error (m)	47.718	50.077	106.079	89.316	67.245

Table 8. Horizontal errors of the GGTRN and combination of GGTRN with profile matching

Traj. no.	GGTRN (centralized + decentralized) (m)	GGTRN (centralized + decentralized) + profile matching (m)	Positional difference (m)	Performance Ratio (%)
1	18.247	16.521	-1.726	110.446
2	15.094	19.481	3.770	77.483
3	12.104	16.872	4.768	71.742
4	13.577	16.081	1.862	84.431
5	16.007	12.588	-2.536	127.158
6	14.967	14.034	-0.933	106.648
7	15.929	18.605	2.833	85.618
8	46.130	14.505	-30.437	318.034
9	27.560	21.654	-5.453	127.278
Average	19.957	16.704	-3.095	119.473

trajectories improved from 19.957m to 16.704m, and the ratio is about 120%, so that the effect of combining EKF with profile matching is meaningful. In particular, eight trajectories (except for trajectory 9) have a horizontal error smaller than 20m, and those are consistent. Thus, it could be said that stability without regional performance ups and downs, which is pursued in this study, was met.

For reference, the average horizontal error in the combination of GGTRN (centralized) and profile matching was about 17.885m. It is not a significant improvement numerically, but the average of 1.2m was updated in this study. Thus, it could be judged that an update of the filter-based algorithm and the combination strategy had a positive effect.

To check the effect of the new combination method in detail, the horizontal error in trajectory 8, which showed the largest improvement, was plotted. In Fig. 2(a), the height of the terrain was lower than 100m for about 100 seconds when the flight had just started, and the flight moved over a plain again after 300 seconds. Because of those significant low variations, the horizontal error increased in TRN. From 100 seconds to 300 seconds, the horizontal error decreased for a while due to variation in the terrain, but it dramatically increased again after 300 seconds. This means that INS errors were not properly compensated for over the plain. On the other hand, the gravity gradient (N-E component) changed similar to a sine curve. Although the range of variations was not that large, it was found that gravity gradient continuously changed as time went on. That is why the horizontal error in GGRN did not increase a lot at the beginning, and the INS error was bound to smaller than a few hundred meters when gravity gradient varied a lot (after 700 seconds). Thus, the overall performance, which was calculated as the standard deviation of the position difference compared to the true trajectory was calculated to be at the 100m level. In this study, GGTRN was modified to combine GGRN and TRN by average, or to apply a centralized solution with an adjusted P matrix. If all geophysical information is combined in a filter, the effect of the gravity gradient could be reduced, because the errors from DBs and sensors are relatively high in GGRN. However, intrinsic characteristics could be reserved when GGRN and TRN are separately developed and combined. Also, the degradation of the P matrix prohibits divergence by increasing the ambiguity in the determined position. As a result, gravity gradient had a positive effect on binding the TRN error, and the horizontal position error did not exceed 250m over the whole flight.

In these efforts, the average horizontal error in trajectory 8 was still 46m. However, the horizontal error decreased by combining the profile matching, and the maximum error was not over 100m. That is because a new position with a 50m level of accuracy was suggested through profile matching, and it was sufficient to check the reliability of GGRN and to combine the algorithms. In particular, the terrain variation

was quite small when flight time reached 900 seconds, so that the error of the selected position from profile matching increased. In that situation, a higher weight was allocated to GGTRN, and it prohibits the position from being hauled away after profile matching, so that horizontal error was consistent over the whole trajectory. Also, the effect of combination could be found in Fig. 2 which shows the flight trajectories of centralized GGTRN, decentralized GGTRN, decentralized GGTRN with profile matching.

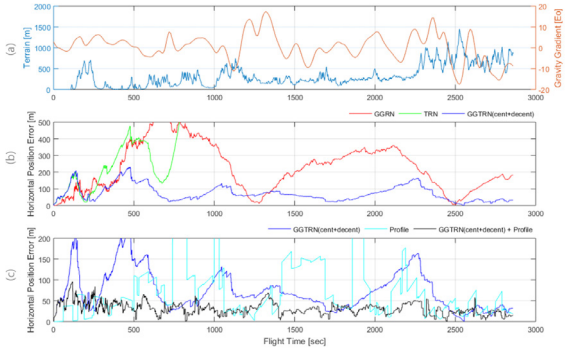

Fig. 2. Variation of Geophysical Data and Horizontal Position Errors of Navigation Algorithms in Trajectory 8: (a) Variation of geophysical data (terrain and gravity gradient), (b) horizontal position errors in GGRN, TRN, and GGTRN, and (c) horizontal position error in GGTRN, profile matching, and the combination of GGTRN and profile matching

With trajectory 3, a significant improvement from the combination of geophysical DBs and algorithms was not found (Fig. 3). Unlike trajectory 8, the terrain changed over the entire trajectory so that the horizontal error was bound to the 11m level in TRN. On the other hand, gravity gradient did not vary a lot. In this situation, over-correction or wrongly calculated correction values from GGRN could have a negative effect on the performance. Also, the 50m level from profile matching performance is not sufficient to complement TRN, which already has about a 10m level of error. However, the horizontal error was calculated to be 17m in the combination algorithm (GGTRN + profile matching), and it is not as big, compared to others. The reason to combine geophysical DBs and the algorithms is to find generalized conditions to guarantee stable performance without regional influence. Thus, it should be emphasized that the updated combination algorithm is meaningful, because all tested trajectories showed consistent navigation results.

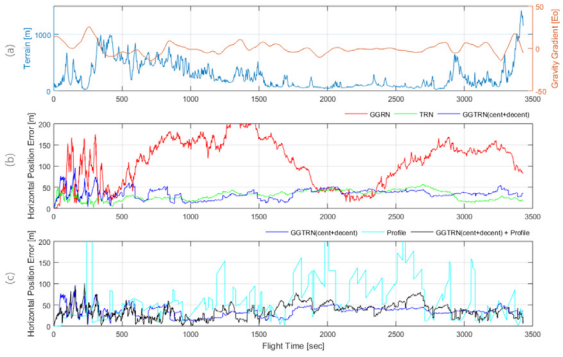

Fig. 3. Variation of Geophysical Data and Horizontal Position Errors of Navigation Algorithms in Trajectory 3: (a) Variation of geophysical data (terrain and gravity gradient), (b) horizontal position errors in GGRN, TRN, and GGTRN, and (c) horizontal position error in GGTRN, profile matching, and the combination of GGTRN and profile matching

4. Conclusions

In this study, a new navigation algorithm was suggested to complement the weakness of geophysical DBs and navigation algorithms and to obtain stable navigation performance. Because geophysical DBs change irregularly, and there is no clear standard to evaluate the reliability of a solution from a navigation algorithm, the new algorithm was developed focusing on finding generalized standards for any test areas. For this reason, GGTRN, which was developed as a type of centralized filter by Lee and Kwon (2016), was modified to switch between a centralized EKF and a decentralized EKF. Also, the final position was determined by combining or switching profile matching with the modified EKF, and the adjusting method for the P matrix was changed from applying a specific value to multiplying a constant to preserve the stability of the P matrix estimated in the filter.

As a result of simulation tests, the average horizontal error from a total of nine trajectories decreased to 19.957m. Considering the 115m and 54m error under GGRN and TRN, it can be concluded that the combination of geophysical DBs and switching the type of filters had a positive effect in terms of stability. In particular, two trajectories where the

vehicle started the flight in a low-variation region diverged under TRN as well as the centralized type of GGTRN, but the horizontal errors of both trajectories were bound to 46m and 27m, respectively.

The final position was determined by combining or switching the modified GGTRN with profile matching. Then, the average horizontal position error over all trajectories decreased to 16.7m, which was about a 3m improvement, compared to the modified GGTRN as applied. Not all trajectories showed improvement compared to the sole geophysical DB solution, to the centralized GGTRN, or to the modified GGTRN, but eight trajectories had a horizontal error smaller than 20m. Although trajectory 9 had a 21.6m error, it is notable because the value is not a big difference, compared to the other trajectories. The effect of the combination filter-based algorithm with profile matching was maximized over a plain. In trajectory 9, TRN and centralized GGTRN diverged, and modified GGTRN showed a horizontal error of about 46m, but the performance improved to 14.50m from the combination of GGTRN and profile matching. Of course, the newly proposed algorithm is not optimal, because some trajectories showed better performance under TRN when the terrain changed a lot over the test area. However, the degradation in the performance was not that big, and the combination algorithm showed a horizontal error smaller than 20m. Thus, it could be concluded that the research objective of deriving a generalized standard was sufficiently achieved because all trajectories generated consistent navigation performance.

Acknowledgment

This research was supported by Basic Science Research Program through the National Research Foundation of Korea(NRF) funded by the Ministry of Education (2016R1A6A3A11932188)

References

Cowie, M., Wilkinson, N., and Powlesland, R. (2008), Latest developments of the TERPROM® digital terrain system (DTS), *Proceedings of IEEE/ION PLANS 2008*, ION, 6-8 May, Monterey, CA, USA, pp. 1219-1229.

Cox, D.B. (1978), Integration of GPS with inertial navigation systems, *Navigations*, Vol. 25, No. 2, pp. 236-245.

Dai, T., Miao, L., and Shao, H. (2019), A robust underwater navigation method fusing data of gravity anomaly and magnetic anomaly, *Inernational Journal of Systems Science*, Vol. 50, No. 4, pp679-693.

DeGregoria, A. (2010), *Gravity Gradiometry and Map Matching: An Aid to Aircraft Inertial Navigation Systems*, Master's thesis, Graduate School of Engineering and Management, Air Force Institute of Technology, Wright-Patterson AFB, OH, USA, 130p.

Groves, P.D. (2013), *Principles of GNSS, Inertial, and Multisensor Integrated Navigation Systems*, Artech house, Boston, MA, USA.

Hollowell, J. (1990), HELI/SITAN: a terrain referenced navigation algorithm for helicopter, *Proceedings of IEEE/ION PLANS 1990*, ION, 20-23 March, Las Vegas, NV, USA, pp. 616-625.

Laur, T.M. and Llanso, S.L. (1995), *Encyclopedia of Modern U.S. Military Weapons*, The Army Times Publishing Company with Berkley Publishing Group, New York, N.Y., USA.

Lee. B. and Kwon, J.H. (2010), Terrain referenced navigation simulation using area-based matching method and TERCOM, *Journal of the Korean Society of Surveying, Geodesy, Photogrammetry and Cartography*, Vol. 28, No. 1, pp. 73-82. (in Korean with English abstract)

Lee, D., Kim, Y., and Bang, H. (2013), Vision-based terrain referenced navigation for unmanned aerial vehicles using homography relationship, *Journal of Intelligent & Robotic Systems*, Vol. 69, No. 1, pp. 489-497.

Lee, J., Kwon, J.H., and Yu. M. (2014), Development of gravity gradient referenced navigation and its horizontal accuracy analysis, *Journal of the Korean Society of Surveying, Geodesy, Photogrammetry and Cartography*, Vol. 32, No. 1, pp. 63-73. (in Korean with English abstract)

Lee, J., Kwon, J.H., and Yu, M. (2015), Performance evaluation and requirements assessment for gravity gradient referenced navigation, *Sensors*, Vol. 15, No. 7, pp. 16833-16847.

Lee, J. and Kwon, J.H. (2016), Analysis of database

referenced navigation by the combination of heterogeneous geophysical data and algorithms, *Journal of the Korean Society of Surveying, Geodesy, Photogrammetry and Cartography*, Vol. 34, No. 4, pp. 373-382.

Lee, W., Yoo, Y.M., Yun, S., and Park, C.G. (2014), Weighting logic design of hybrid database referenced navigation algorithm using multiple geophysical information, *Proceedings of 19th IFAC World Congress*, IFAC, 24-29 August, Cape Town, South Africa, Vol. 47, No. 3, pp. 3407-3412.

Leonard, J.J. and Bahr, A. (2019), Autonomous Underwater Vehicle Navigation, In: (Dhanak, M.R. and Xiros, N.I (eds.), *Springer Handbook of Ocean Engineering*, Springer International Publishing, NY, USA, pp.341-358.

Liu, F., Qian, D., Liu, F., and Li, Y. (2009), Integrated navigation system based on correlation between gravity gradient and terrain, *Proceedings of International Joint Conference on Computational Sciences and Optimization*, IEEE, 24-26 April, Hainan, China, Vol. 2, pp. 289-293.

Liu, F., Qian, D., Zhang, Y., and Li, Y. (2010), A computer simulation of the influence of GGI and inertial sensors on gravity gradient aided navigation, *Proceedings of 2010 International Symposium on Systems and Control in Aeronautics and Astronautics*, ISSCAA, 8-10 June, Harbin, China, pp. 793-797.

Mok, S.H., Band, H.C. and Yu, M.J. (2012), A performance comparison of nonlinear Kalman filtering based terrain referenced navigation, *Journal of the Korean Society for Aeronautical and Space Science*, Vol. 40, No. 2, pp.108-117. (in Korean with English abstract)

Nielson, J.T., Swearingen, G.W., and Witzmeer, A.J. (1986), GPS aided inertial navigation, *Aerospace and Electronic Systems Magazine*, Vol. 1, No. 3, pp.20-26.

Perea, L., How, J., Breger, L., and Elosegui, P. (2007), Nonlinearity in sensor fusion: divergence issues in EKF, modified truncated SOF, and UKF, *Proceedings of AIAA Guidance, Navigation and Control Conference and Exhibit*, AIAA, 20-23 August, Hilton Head, S.C., USA, Vol. 6514.

Richeson, J.A. (2008), *Gravity Gradiometer Aided Inertial Navigation within Non-GNSS Environments*, Ph. D. dissertation, University of Maryland, College Park, MD, USA, 405p.

Robins, A. (1998), Recent developments in the 'TERPROM' integrated navigation system, *Proceedings of the ION 44th Annual Meeting*, ION, 21-23 June, Annapolis, MD, USA, pp. 58-66.

Rogers, M.M. (2009), *An Investigation into the Feasibility of Using a Modern Gravity Gradient Instrument for Passive Aircraft Navigation and Terrain Avoidance*, Master's thesis, Graduate School of Engineering and Management, Air Force Institute of Technology, Wright-Patterson AFB, OH, USA, 164p.

Skog, I. (2009), *Low-Cost Navigation Systems: A Study of Four Problems*, Ph.D. dissertation, KTH Royal Institute of Technology, Stockholm, Sweden, 165p.

Stutters, L., Liu, H., Tiltman, C., and Brown, D.J. (2008), Navigation technologies for autonomous underwater vehicles, *IEEE Transactions on Systems, Man, and Cytermetrics*, Part C, Vol. 38, No. 4, pp.581-589.

Wang, B., Yu, L., Deng, Z., and Fu, M. (2016), A particle filter-based matching algorithm with gravity sample vector for underwater gravity aided navigation, *IEEE/ASME Transactions on Mechatronics*, Vol. 21, No. 3, pp.1399-1408.

Wang, Z. and Bian, S. (2008), A local geopotential model for implementation of underwater passive navigation. *Progress in Natural Science*, Vol. 18, No. 9, pp. 1139-1145.

Xiong, L., Xiao, L.W., Dan, B.B., and Ma, J. (2013), Full tensor gravity gradient aided navigation based on nearest matching neural network, *Proceedings of Cross Strait Quad-Regional Radio Science and Wireless Technology Conference*, IEEE, 21-25 July, Chengdu, China, pp. 462-465.

Yu, Y.M., Yu, M.J., and Park, C.G. (2013), Research trend of terrain referenced navigation system, *Institute of Control, Robotics and Systems*, Vol. 19, No. 1, pp.19-31.

Yurong, H., Bo, W., Zhihong, D., and Mengyin, F. (2018), Point mass filter based matching algorithm in gravity aided underwater navigation, *Journal of Systems Engineering and Electonics*, Vol. 29, No. 1, pp.152-159.

Zhang, F., Chen, X., Sun, M., Yan, M., and Yang, D. (2004), Simulation study of underwater passive navigation system based on gravity gradient, *Proceedings of International Geoscience and Remote Sensing Symposium*, IEEE, 20-24 September, Anchorage, AK, USA, Vol. 5, pp. 3111-3113.